Strong ionisation in carbon nanowires

V. Kaymak, A. Pukhov, V.N. Shlyaptsev, J.J. Rocca

Abstract. **Surfaces covered with nanostructures, such as nanowire arrays, are shown to facilitate a significantly higher absorption of laser energy as compared to flat surfaces. Due to the efficient coupling of the laser energy, highly energetic electrons are produced, which in turn can emit intense ultrafast X-ray pulses. Full three dimensional PIC simulations are used to analyse the behaviour of arrays of carbon nanowires 400 nm in diameter, irradiated by a 400-nm laser pulse of 60-fs duration at FWHM and a vector potential of $a_0 = 18$. We analyse the ionisation dynamics of the nanowires. The difference of the ionisation strength and structure between linearly and circularly polarised laser beam is investigated. The nanowires are found to be fully ionised after about 30 laser cycles. Circularly polarised light reveals a slightly stronger ionisation effect.**

1. Introduction

High-intensity lasers can heat solid density plasmas to high temperatures. The formation of a highly conductive plasma surface will, however, limit the penetration depth to a thin surface layer. Most of the laser light is therefore reflected. There are two different approaches to overcome this obstacle: generating a preplasma (by using a prepulse) or structuring the irradiated surface [1].

Arrays of nanoparticles such as nanowires have been shown to facilitate a high absorption of the laser light. They typically have a high average density and a high (solid) local density. The efficient coupling of the laser energy to the material can be attributed to locally enhanced electric fields in the vicinity of the nanoparticles. Two mechanisms cause the enhancement: the so-called 'lighting rod' effect, which is a purely geometric factor depending on the shape of the particle, and surface plasmon resonances [2].

V. Kaymak, A. Pukhov Institut für Theoretische Physik, Heinrich-Heine-Universität Düsseldorf, 40225 Düsseldorf, Germany;
e-mail: vural.kaymak@tpl.uni-duesseldorf.de;
V.N. Shlyaptsev Department of Electrical Computer Engineering, Colorado State University, Fort Collins, Colorado 80523, USA;
J.J. Rocca Department of Electrical Computer Engineering, Colorado State University, Fort Collins, Colorado 80523, USA
Department of Physics, Colorado State University, Fort Collins, Colorado 80513, USA

Due to the high absorption of the laser energy, highly energetic electrons are produced, which can emit X-ray pulses [3] of down to subpicosecond duration [4] of up to several hundred keV [5]. Designed as tabletop pulsed X-ray sources they can allow one to follow processes on the atomic and molecular timescale [6]. Other fields of application of laser-produced plasmas are accelerated MeV ions [7] and the generation of fusion neutrons [8].

2. Simulation setup

In the present work we use full three dimensional PIC simulations with the Virtual Laser Plasma Lab (VLPL) Code [9]. The simulation setup contains a carbon nanowire of 400 nm diameter and 5 μm length. Their periodicity is 1 μm, which corresponds to an average density of the wires of 13 % solid density. A laser pulse of 60 fs FWHM duration and a vector potential of $a_0 = 18$ is injected into the simulation box and irradiates the nanowire.

The laser beam is modelled as a plane wave with a Gaussian temporal profile impinging at normal incidence (see Fig. 1). The simulation box contains only a single rod, periodic boundary conditions in transverse direction simulating an array of nanowires. In the propagation direction (both left and right) the boundaries are absorbing to make sure that there is no reflected pulse interacting again with the nanowire. The code incorporates field and collisional ionisation as well as binary collisions.
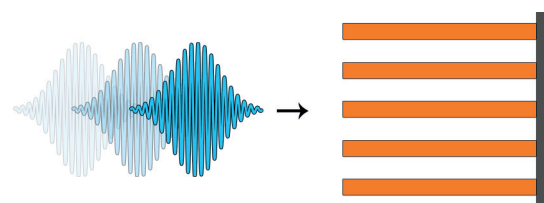

Figure 1. Scheme of the simulation setup.

3. Ionisation process

We will first consider how the laser pulse penetrates into the nanowire and ionises it along the wire axis. To point out how differently a linearly and circularly polarised laser pulse influences the process, we subsequently consider the ionisation in the plane perpendicular to the wire axis. The electrons which are removed from the carbon ions this way turn out to be pulled out of the nanowire, moving under the influence of the electric field.

3.1. Ionisation structure along the wire axis

Figure 2 shows the time evolution of the longitudinal cross section (in the xy plane) of the electron charge density ρ_e.

The laser pulse, entering the simulation box from the left boundary at $x = 0$, clearly penetrates the nanowire. The carbon ions initially have an ionisation state with a charge number $Z = 1$, leading to a charge density of about $\rho_e \approx 16en_{cr}$ (bright gray area in Fig. 2). The tip of the wire starts to get ionised (Fig. 2a) and the charge density increases to about $\rho_e \approx 60en_{cr}$. It can be seen that the outer layer of the wire is ionised first (see, for example, the right end of the ionised area in Figs 2a–2c). Only after that, since there is also collisional ionisation, the ionisation reaches the inner core at the wire axis. Even before the whole wire has gained a minimum charge density of about $\rho_e \approx 60en_{cr}$, the left half of the wire already gets ionised to values of about $90en_{cr}$ (Figs 2c and 2d). For Figs 2a–2d a linearly polarised laser was used. In principle these cross sections do not change for circular polarisation. However, thi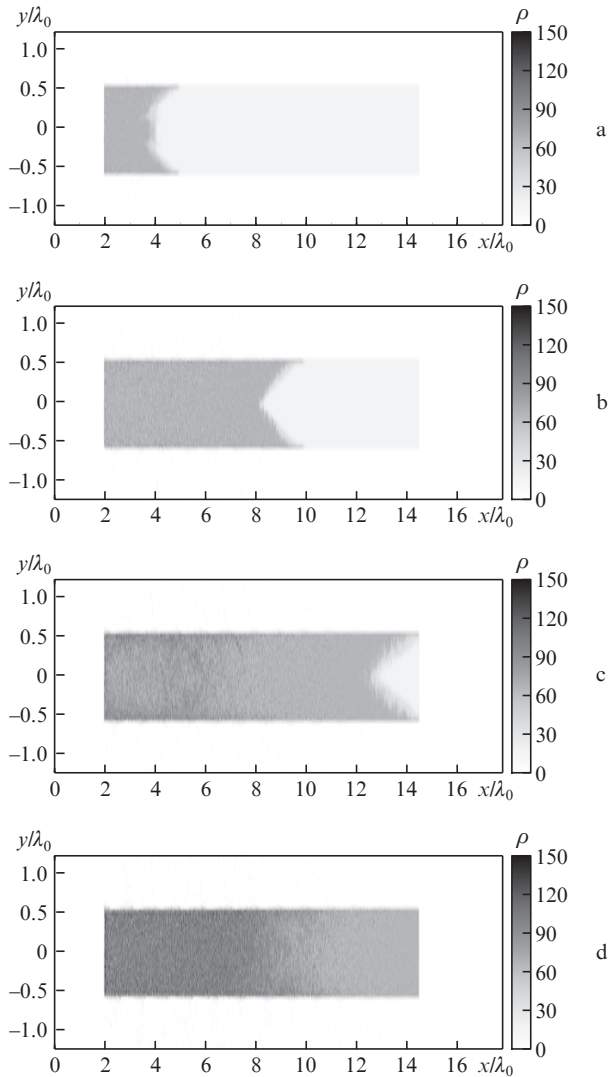s does not preclude that the ionisation structure may be different. A more direct way to observe the ionisation strength is to consider the (averaged) ionisation state (charge number Z) of the carbon ions along the whole nanowire (see Fig. 3). They provide a direct comparison between the ionisation by a linearly polarised laser beam (Fig. 3a) and a circularly polarised laser beam (Fig. 3b) at four different times.
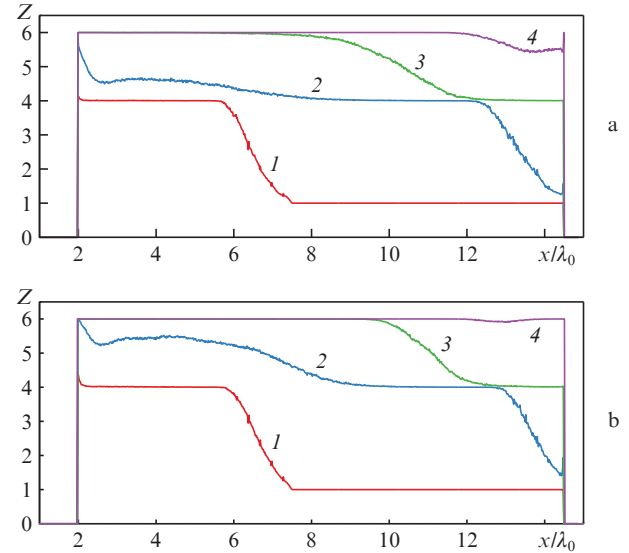

Figure 3. Averaged ionisation state Z of the carbon ions along the wire axis x for a (a) linearly polarised and (b) circularly polarised laser pulse at $t = (1) -48.5T_0$, (2) $-41T_0$, (3) $-33.5T_0$ and (4) $-26T_0$.

At the first time step ($t = -48.5T_0$) the curves for linear and circular polarisations mostly coincide. The carbon wire is fourfold ionised up to $3.5\lambda_0$ into the tip and falls to the initial state of $Z = 1$ within a length of $2\lambda_0$. After 7.5 laser cycles, the state $Z = 4$ reaches up to $10\lambda_0$ into the wire for linear polarisation and $10.7\lambda_0$ for circular polarisation. Whereas the interval $2.5\lambda_0 < x < 9\lambda_0$ has averaged charged states up to $Z = 4.6$ for the linear polarisation, the circular polarisation reaches higher states of up to $Z = 5.5$. At $t = -33.5T_0$ the first $5\lambda_0$ laser wavelengths of the wire (linear polarisation) and $7.5\lambda_0$ (circular polarisation) are fully ionised. At the last step ($t = -26T_0$) the wire is basically fully ionised by the circularly polarised beam. In the case of linear polarisation, the last $2.5\lambda_0$ laser wavelengths have charge states between 6 and 5.5.

3.2. Ionisation structure in the transverse plane

Consideration of the transverse plane of the wire axis gives a further insight into the structure of the ionisation. Figure 4 shows the averaged (along the x axis) ionisation state in the yz plane for linear polarisation (in y direction). The white area surrounding the wire stands for empty space. Figure 4a shows how the surfaces of the wire intersecting with the polarisation direction going through the wire centre carry higher ionisation states (of about 4.4) than the rest of the rod. This is strong evidence that the surfaces crossing the electric field vector are ionised first. In the next step, the ionising effect goes deeper into the bulk of the wire (Fig. 4b). Due to the linear polarisation, the area of high charge states (~5.4) goes along the y direction through $x = 0$. Gradually a fully ionised plasma forms in that area (Fig. 4c) until it covers the entire rod and starts to expand (Fig. 4d).
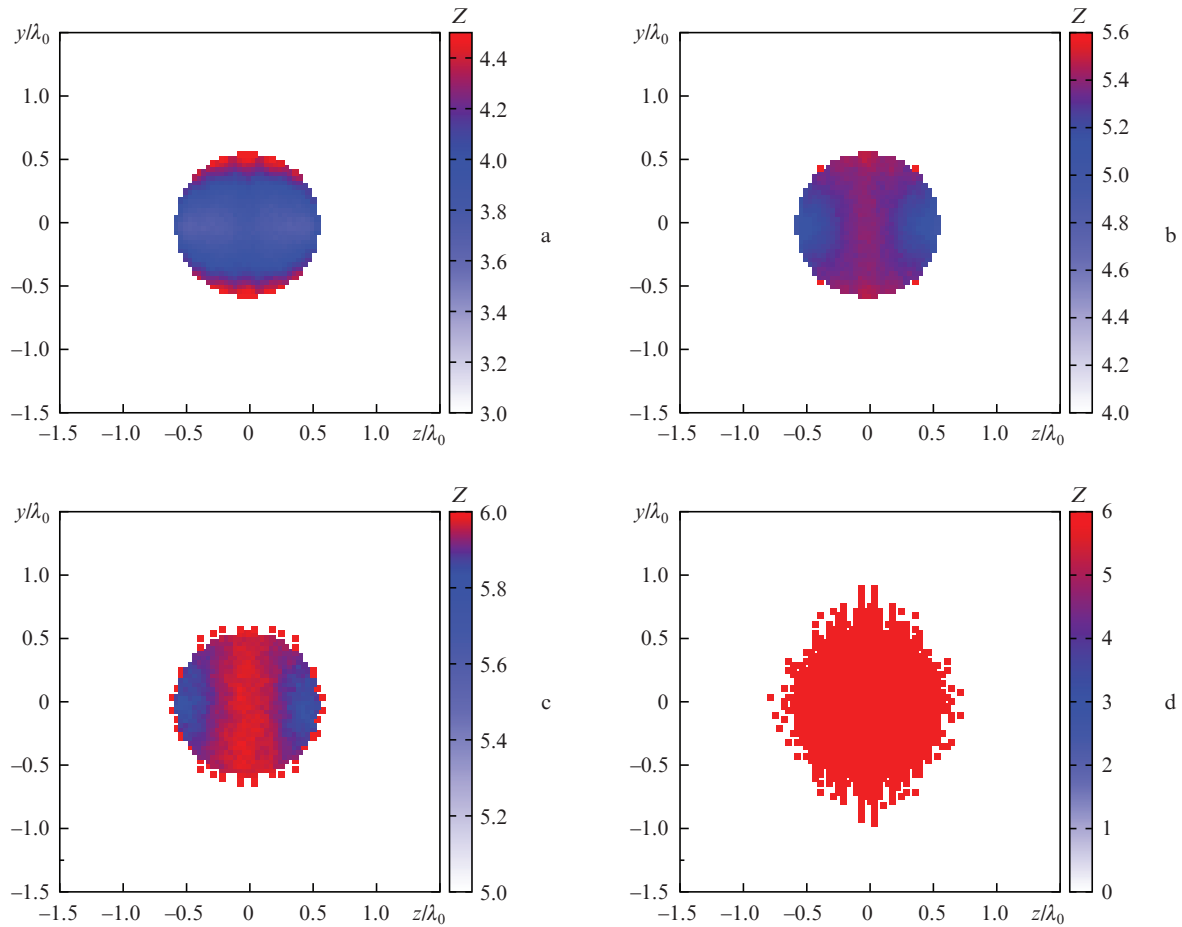

Figure 2. Longitudinal (cut along $z = 0$) cross sections of the electron charge density $\rho = \rho_e/(en_{cr})$ at $t = $ (a) $-51T_0$, (b) $-46T_0$, (c) $-41T_0$ and (d) $-36T_0$ before the peak of the (linearly polarised) laser pulse (in the y direction) hits the surface; T_0 is the laser cycle.

Figure 4. (Colour online) Distributions of the averaged ionisation state Z of the carbon ions at $t =$ (a) $-41T_0$, (b) $-33.5T_0$, (c) $-26T_0$ and (d) $-18.5T_0$ before the peak of the (linearly polarised) pulse hits the surface. The colour scale has been adapted in order to make the difference of the charged states visible.

This ionisation structure is slightly different for a circularly polarised pulse (Fig. 5). At first, it is obvious that there is no preferred direction of the ionised surface areas (Fig. 5a). The surface is rather uniformly ionised over the whole circle. In the next step at $t = -33.5T_0$ the charge states are uniformly distributed along the cross section. While for linear polarisation at $t = -26T_0$ the wire has areas with a charge of about $Z = 5.8$, Fig. 5c reveals a basically fully ionised wire. As before, the wire eventually expands (Fig. 5d).

3.3. Void electrons

In the previous subsection we have seen that the nanowire is firstly ionised at the surface. As one could assume, the electrons that are removed from the carbon ions are pulled out of the wire into the voids. The structure of the arrangement of those electrons is a trace of the electric field vector. Thus, they are ordered in the polarisation plane for linear polarisation. On the other hand, the released electrons are arranged on a spiral around the wire along the x axis when irradiated by a circular polarised pulse. In order to see the periodicity of those electronic structures, one can employ cross sections of the current density distributions j_y and j_z as shown in Fig. 6. The current density components j_y and j_z illustrate the flow of electrons in the plane perpendicular to the wire axis. Figure 6a confirms that there are currents in the gaps of

the wires with a periodicity of one laser wavelength that move upwards and downwards along the polarisation axis.

This becomes clear in the presentation of the j_y component. However, there is no such periodic structure in the j_z component. On the other hand, there are currents that are uniform along both y and z directions, as can be seen by comparing the corresponding j_y and j_z distributions in the case of circular polarisation (Fig. 6b). One can notice that for both polarisations these currents are restricted to the surrounding of the wire bulk since there are no visible periodic structures inside the nanowire.

4. Conclusions

We have investigated the ionisation in laser irradiated arrays of carbon nanowires. It turns out that the strong laser pulse fully ionises the nanowire within a time of about 30 laser cycles. We have seen how the wires are ionised along the wire axis and that a circularly polarised pulse has a slightly stronger ionising effect. We have found that the outer layers of the nanowire are ionised first with a structure determined by the polarisation. Moreover, we have shown that there are periodical transverse currents in the surrounding of the wire transporting electrons to the voids.

Further studies are required to investigate how the ionisation is influenced by the wire properties as for instance the
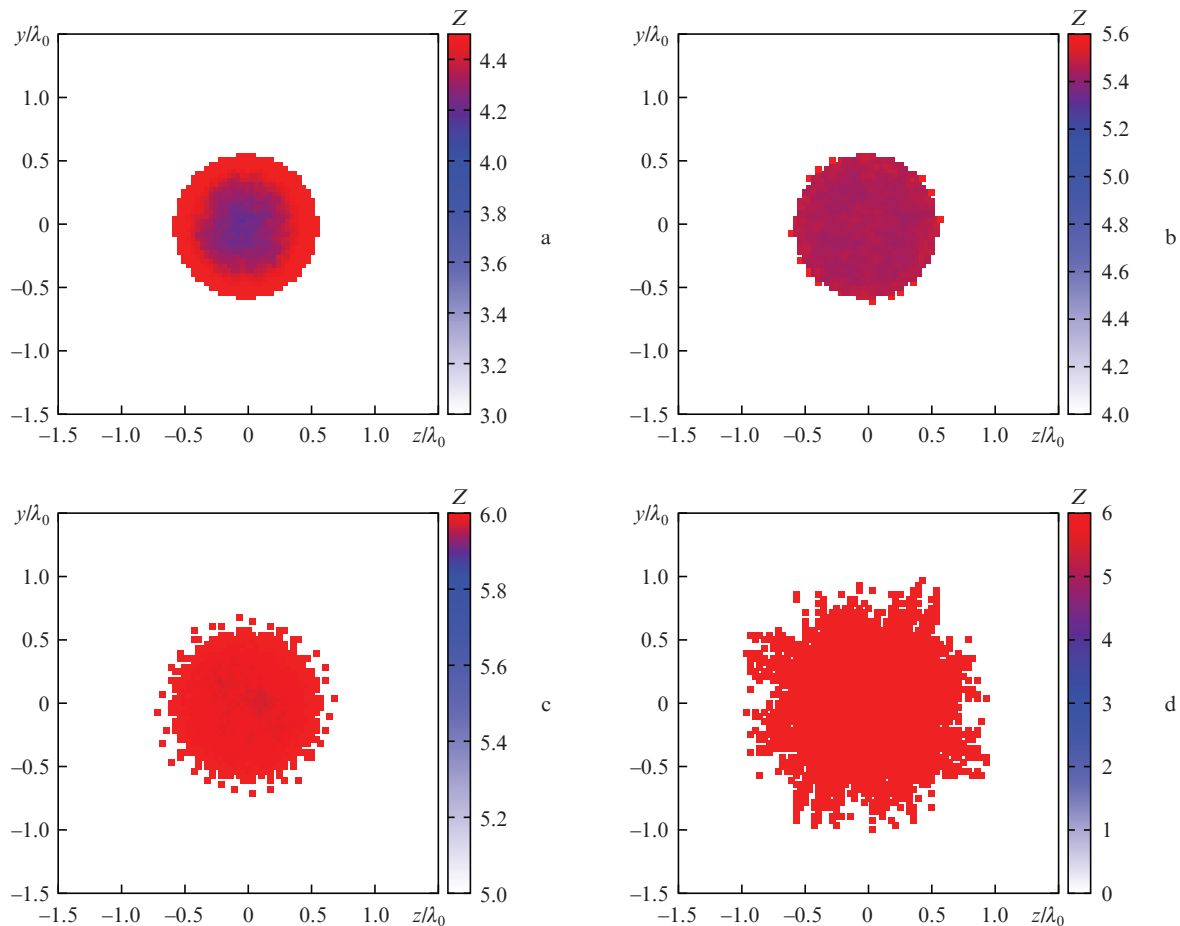
Figure 5. (Colour online) Distributions of the averaged ionisation state Z of the carbon ions at $t =$ (a) $-41T_0$, (b) $-33.5T_0$, (c) $-26T_0$ and (d) $-18.5T_0$ before the peak of the (circularly polarised) pulse hits the surface. The colour scale has been adapted in order to make the difference of the charged states visible.
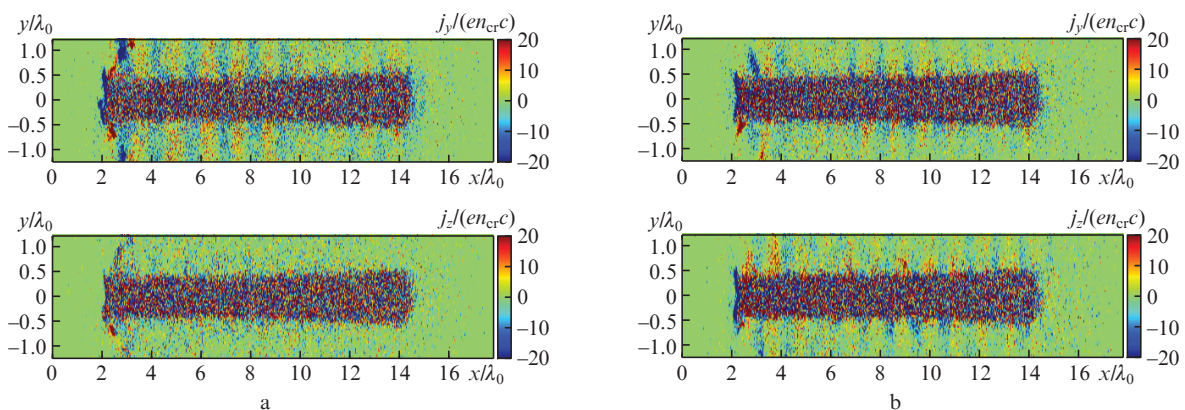

Figure 6. (Colour online) Longitudinal cross sections (in the xy plane) of current density components $j_y/(en_{cr}c)$ and $j_z/(en_{cr}c)$ at $t = 4T_0$ after the peak of the pulse hits the surface for a (a) linearly polarised and (b) circularly polarised laser.

diameter, the length, the periodicity and the nanowire material. Also a variation of the laser parameters like the intensity could give more insight to the ionisation process in nanowires.

References

1. Nishikawa T., Nakano H., Oguri K., Uesugi N., Nakao M., Nishio K., Masuda H. *Appl. Phys. B*, **73**, 185 (2001).
2. Rajeev P.P., Ayyub P., Bagchi S., Kumar G.R. *Opt. Lett.*, **29**, 2662 (2004).
3. Purvis M.A., Shlyaptsev V.N., Hollinger R., Bargsten C., Pukhov A., Prieto A., Wang Y., Luther B., Yin L., Wang S., Rocca J. *Nat. Photonics*, **7**, 796 (2013).

4. Dorchies F., Blasco F., Bonté C., Caillaud T., Fourment C., Peyrusse O. *Phys. Rev. Lett.*, **100**, 205002 (2008).
5. Mondal S., Chakraborty I., Ahmad S., Carvalho D., Singh P., Lad A.D., Narayanan V., Ayyub P., Ravindra Kumar G., Zheng J., Sheng Z.M. *Phys. Rev. B*, **83**, 035408 (2011).
6. Gibbon P., Förster E. *Plasma Phys. Control. Fusion*, **38**, 769 (1996).
7. Zigler A., Palchan T., Bruner N., Schleifer E., Eisenmann S., Botton M., Henis Z., Pikuz S.A., Faenov A.Y. Jr, Gordon D., Sprangle P. *Phys. Rev. Lett.*, **106**, 134801 (2011).
8. Ditmire T., Zweiback J., Yanovsky V.P., Cowan T.E., Hays G., Wharton K.B. *Nature*, **398**, 489 (1999).
9. Pukhov A. *J. Plasma Phys.*, **61**, 425 (1999).